Biochimica et Biophysica Acta 1807 (2011) 243–250

Contents lists available at ScienceDirect

Biochimica et Biophysica Acta

journal homepage: www.elsevier.com/locate/bbabio

Inhibition of Photosystem II by the singlet oxygen sensor compounds TEMP and TEMPD

Marja Hakala-Yatkin, Esa Tyystjärvi *

Molecular Plant Biology, Department of Biochemistry and Food Chemistry, FI-20014 University of Turku, Finland

ARTICLE INFO

Article history:
Received 28 June 2010
Received in revised form 12 November 2010
Accepted 24 November 2010
Available online 2 December 2010

Keywords:
Photosystem II
Photoinhibition
Singlet oxygen
Thermoluminescence
2,2,6,6-tetramethylpiperidine
2,2,6,6-tetramethyl-4-piperidinone

ABSTRACT

2,2,6,6-tetramethylpiperidine (TEMP) and 2,2,6,6-tetramethyl-4-piperidinone (TEMPD) have earlier been used to quantify singlet oxygen produced by plant material. Both compounds were found to cause severe side effects on Photosystem II. Addition of TEMP or TEMPD to thylakoids immediately stabilized the reduced state of the Q_A electron acceptor and destabilized the reduced state of the Q_B acceptor, causing decrease in the driving force of forward electron transfer. Oxygen evolution, thermoluminescence and fluorescence measurements indicated that the number of functional PSII units decreased during incubation of thylakoids with TEMP or TEMPD. Singlet oxygen determinations in photosynthetic systems with piperidine derivatives should be interpreted with care.

1. Introduction

Reaction between singlet oxygen ($^1O_2$) and certain piperidine derivatives like 2,2,6,6-tetramethylpiperidine (TEMP) [1] and 2,2,6,6-tetramethyl-4-piperidinone (TEMPD) produce the respective nitroxides that can be quantified with electron paramagnetic resonance spectroscopy (Fig. 1). The specificity of TEMP and TEMPD to $^1O_2$ has promoted the use of these compounds for detection of $^1O_2$ from biological material. TEMPO, the nitroxide product of TEMP, and various derivatives of TEMPO, are widely used in synthetic chemistry and also as radical traps in life sciences [2,3].

In plants, $^1O_2$ is produced mainly by Photosystem II (PSII) [4–10]. PSII is also the target of light-induced inactivation termed photoinhibition (for reviews, see [11–14]). Both visible and ultraviolet light cause photoinhibition but ultraviolet light is much more efficient.

Many of the hypotheses about the mechanism of photoinhibition suggest that $^1O_2$ has a role in the reaction. In the historical acceptor-side hypothesis [15], protonation or double reduction of the Q_A electron acceptor in strong light leads to enhanced production of the triplet state of the primary radical pair, and consequently to production of $^1O_2$. The acceptor-side hypothesis is supported by the finding that the percentage of photoinhibited PSII centers correlates with the amount of $^1O_2$ produced by leaves [6]. On the other hand, occurrence of photoinhibition under anaerobic conditions [15,16] supports the independence of photoinhibition of $^1O_2$. In some photoinhibition hypotheses, $^1O_2$ has a direct inhibitory role. It has been suggested that $^1O_2$ produced by recombination of the primary radical pair in the presence of unprotonated Q_A^- causes photoinhibition [14]. Experiments in which photoinhibition was induced with short laser pulses led to the suggestion that even the triplet chlorophyll produced by the slow charge recombination reactions between the quinone acceptors and the oxygen evolving complex may induce enough $^1O_2$ to cause measureable photoinhibition of PSII in low light [17]. $^1O_2$ produced by weakly coupled chlorophylls [18] or by iron–sulfur centers and cytochromes [19] has also been suggested to cause photoinhibition.

Photoinhibition hypotheses in which the inhibition occurs primarily on the donor side of PSII do not have explicit connections to $^1O_2$. In the classical donor-side hypothesis [20,21], photoinhibition occurs when P_{680}^+ is not normally reduced by the oxygen evolving complex. In the manganese hypothesis [22,23], photoinhibition is triggered by light absorption by the manganese ions themselves, which leads to inhibition of oxygen evolution and also to further damage by P_{680}^+. The occurrence of manganese-based photoinhibition is supported by several lines of evidence, including action spectra [22,23], low protective efficiency of quenching of chlorophyll excitations [24,25], results from photoinhibition in UV-A light [26,27], similarity of the quantum yield of photoinhibition induced with single-turnover flashes and with continuous light [28], and photosensitivity of manganese model compounds [29,30].

Abbreviations: Chl, Chlorophyll; DCMU, 3-(3,4-dichlorophenyl)-1,1-dimethylurea; DCBQ, 2,6-dichloro-p-benzoquinone; F_V/F_M, ratio of variable to maximum Chl *a* fluorescence; $^1O_2$, singlet oxygen; PSII, Photosystem II; TEMP, 2,2,6,6-tetramethylpiperidine; TEMPD, 2,2,6,6-tetramethyl-4-piperidinone; TL, thermoluminescence

* Corresponding author. Tel.: +358 40 511 3503; fax: +358 2 333 5549.
E-mail address: esatyy@utu.fi (E. Tyystjärvi).

0005-2728/$ – see front matter © 2010 Elsevier B.V. All rights reserved.
doi:10.1016/j.bbabio.2010.11.014

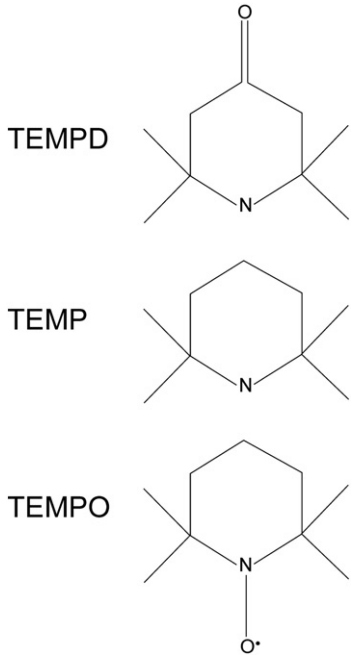

Fig. 1. Structures of TEMPD, TEMP and the TEMPO radical which is the product of the reaction between TEMP and $^1O_2$.

Measurements of $^1O_2$ production in chloroplasts require that the sensor compounds do not interfere with PSII, but there has been little interest in measuring potential side effects. The aim of the present study was to test if TEMP or TEMPD affect PSII electron transport. Pumpkin thylakoids were treated with TEMP or with TEMPD, using concentrations applied to measure $^1O_2$. Oxygen evolution, ratio of variable to maximum chlorophyll (Chl) *a* fluorescence (F_V/F_M), decay of fluorescence yield after a single turnover flash and thermoluminescence (TL) were measured to analyze the effects of the compounds.

2. Materials and methods

2.1. Incubation of thylakoids with TEMP and TEMPD

Thylakoid membranes were isolated from pumpkin (*Cucurbita maxima*) leaves as earlier described [22]. Thylakoid incubations with TEMP and TEMPD were done at room temperature in the dark in buffer containing 40 mM HEPES-KOH (pH 7.6), 0.3 M sorbitol, 5 mM $MgCl_2$, 5 mM NaCl and 1 M glycine betaine. On the basis of literature describing the use of TEMP and TEMPD for $^1O_2$ detection, we used TEMP at 10 mM [31] and TEMPD at 100 mM concentration [32]. Chl concentration during the incubation was 20 μg ml^{-1} in oxygen evolution and fluorescence experiments and 1 mg ml^{-1} in the TL experiments.

2.2. Measurements of oxygen evolution and fluorescence

The light-saturated rate of oxygen evolution was measured with an oxygen electrode (Hansatech, King's Lynn, GB) using 0.125 mM 2,6-dichloro-p-benzoquinone (DCBQ) as electron acceptor. F_V/F_M was measured with PAM-101 fluorometer (Walz, Effeltrich, Germany). F_0 was measured using a dim measuring beam alone and F_M was measured with a saturating light pulse (5000 μmol photons m^{-2} s^{-1}). The decay of Chl *a* fluorescence yield after a single turnover flash was measured with FL3500 fluorometer (Photon System Instruments, Brno, Czech Republic). DCMU-induced increase in F_0 fluorescence was measured by first measuring a continuous, stable F_0 level in thylakoids with the PAM fluorometer, then adding DCMU to a final concentration of 10 μM and following the fluorescence induced by the dim measuring beam for the total time of 2 min.

2.3. TL measurements

TL was measured with a luminometer described earlier [33]; see [34] for a review of TL instrumentation. Thylakoids were incubated with TEMP or TEMPD, and TL was measured from 120 μl aliquots. To measure the B band of TL, the thylakoid sample was diluted to 0.75 mg Chl ml^{-1} by addition of buffer and cooled to 0 °C. A 1 J Xenon flash was fired, and the sample was then immediately heated at the rate of 1 °C s^{-1} to 65 °C. For the Q band measurements, 20 μM 3-(3,4-dichlorophenyl)-1,1-dimethylurea (DCMU) and 25% glycerol were added and the sample was cooled to −15 °C, a flash was fired and the sample was then heated at 1 °C s^{-1} to 65 °C. Glycerol was used in Q band measurements to avoid artefacts due to the melting of the sample, and the samples were kept small and concentrated in order to achieve temperature homogeneity [34]. The TL signal was digitized at the rate of 10 samples/s and smoothened by calculating a moving average with a 3.5 °C window. Three independent replicate TL curves were always averaged and a background signal, averaged from three nonflashed samples, was subtracted from each TL curve.

2.4. Analysis of TL and fluorescence data

All TL data were analyzed by assuming that the luminescence intensity is always proportional to the rate of a luminescence-producing recombination reaction [35,36] and that the rate constants of the recombination reactions can be calculated from the Eyring equation [37]. In modeling the Q band reflecting the reaction $S_2Q_A^- \rightarrow S_1Q_A$, it was assumed [35,36] that $S_2Q_A^-$ recombines via three competing routes: (i) direct recombination of Q_A^- with P_{680}^+, (ii) indirect recombination via the intermediate formation of $P_{680}^+Pheo^-$ and subsequent nonradiative decay to the ground state, and (iii) excitonic route in which the excited state P_{680}^* is an intermediate and luminescence emission may occur. The energetic connectivity of PSII was taken into account [33] in modeling the excitonic route. In addition, it was assumed that PSII consists of a main slowly-recombining population and a minor rapidly recombining population with the same activation enthalpies for all three pathways but different activation entropies. This assumption is equivalent with the assumption that the three pathways have the same activation energies in the two populations but the rate constants have different preexponential factors of the Arrhenius theory [35,36]. Thus, the decrease of the concentration of $S_2Q_A^-$ as a function of time (t) was fitted with the following equation

$$[S_2Q_A^-] = [S_2Q_A^-]_{0,slow} e^{-(k_{i,slow} + k_{exc,slow} + k_{d,slow})t} + [S_2Q_A^-]_{0,fast} e^{-(k_{i,fast} + k_{exc,fast} + k_{d,fast})t}, \quad (1)$$

where k_i, k_{exc} and k_d are the rate constants of the three reaction routes and slow and fast refer to the two populations of PSII. According to the Eyring theory, each rate constant can be expressed as follows

$$k_{\{i/exc/d\},\{slow/fast\}} = \frac{k_b T}{h} e^{\frac{\Delta S^{\ddagger}_{\{i/exc/d\},\{slow/fast\}}}{k_b}} e^{-\frac{\Delta H^{\ddagger}_{\{i/exc/d\}}}{k_b T}}, \quad (2)$$

where k_b is Boltzmann's constant, h is Planck's constant, T is temperature and the subscripts {i/exc/d} and {slow/fast} indicate constants belonging to the indirect, excitonic or direct pathway of the slow or the fast population of PSII, respectively. Thermoluminescence intensity I was assumed to be proportional to the sum of the rates of the excitonic routes of the slow and the fast population of PSII,

corrected for the effect of the energetic connectivity of PSII [33] as follows

$$I(t) = c\left\{A_{slow}\frac{k_b}{h}(T_0+\beta t)e^{\frac{\Delta S^{\ddagger}_{exc,slow}}{k_b}}e^{-\frac{\Delta H^{\ddagger}_{exc}}{k_b(T_0+\beta t)}} + A_{fast}\frac{k_b}{h}(T_0+\beta t)e^{\frac{\Delta S^{\ddagger}_{exc,fast}}{k_b}}e^{-\frac{\Delta H^{\ddagger}_{exc}}{k_b(T_0+\beta t)}}\right\}(1-q)\frac{1+J}{1+qJ}, \quad (3)$$

where c is a scaling constant, A_{slow} and A_{fast} are the initial fractions of the slow and fast PSII populations, T_0 is the temperature (K) at which the heating starts, β is the heating rate, q is the fraction of open PSII reaction centers, calculated from the time-course of TL, and J is a parameter describing the energetic connectivity of PSII [38,39]. The beginning of the heating was used as the time point zero, and in the final data, time was replaced with temperature T according to the equation $T = T_0 + \beta t$.

The recombination reaction $S_2Q_B^- \rightarrow S_1Q_B$ which produces the B band of TL in the absence of DCMU, was analyzed as a single first-order band, i.e. using Eq. (1) without the correction factor $(1-q)(1+J)/(1-qJ)$.

The decay of Chl *a* fluorescence yield after a single turnover flash in the presence of DCMU was analyzed with the same model as TL (Eqs. (1)–(2)) at constant temperature and assuming that variable fluorescence is proportional to the fraction of reduced Q_A. A correction for the effect of the energetic connectivity of PSII was done with the connectivity parameter J as follows [38,39]

$$\frac{F_V}{F_M - F_0} = \frac{1-q}{1+qJ}. \quad (4)$$

Although the same model, based on activation parameters of the reactions rather than the rate constants, was used for analysis of fluorescence and TL, only the total rate constant of the decay of the $S_2Q_A^-$ state in the two PSII populations will be reported from fluorescence, as measurements at one temperature do not allow separation of the activation parameters of the three pathways.

Variable fluorescence yield obtained with a single-turnover pulse is considerably lower than the maximum F_V obtained with a multiple-turnover pulse (see [39]). The maximum value of F_V ($=F_M - F_0$) was measured separately from similar samples by firing the single-turnover pulses at 1 ms intervals in the presence of DCMU until the increase in fluorescence yield stabilized. An ultra-slow decay component, not kinetically resolved by the 160-s long fluorescence measurement, was added as a constant fluorescence value.

The decay of fluorescence yield after a single turnover flash in the absence of DCMU was modeled by assuming that PSII exists in states $Q_A^-Q_B$, $Q_A^-Q_B^-$, $Q_A^-Q_BH_2$ and Q_A^- with an empty Q_B site (Q_A^-E) plus a population of inactive PSII centers in which a recombination reaction ($S_2Q_A^- \rightarrow S_1Q_A$) occurs instead of forward electron transfer. For the active centers, the model assumed reactions (i) $Q_A^-Q_B \rightarrow Q_AQ_B^-$, (ii) $Q_A^-Q_B^- \rightarrow Q_AQ_B^{2-}$, (iii) $Q_A^-E \rightarrow Q_A^-Q_B$, and (iv) $Q_A^-Q_BH_2 \rightarrow Q_AE$. Reactions (i) and (ii) are known to have submillisecond time constants while reaction (iii) occurs in the time domain of several milliseconds [36,40]. The larger of the submillisecond rate constants was assigned to reaction (i). All reactions were assumed to be of first order. Correction for the energetic connectivity of PSII was done in the same way as was done in the presence of DCMU. The ModelMaker software (Cherwell Scientific Ltd., Oxford, UK) was used for all numerical modeling.

3. Results

To measure the effects of TEMP and TEMPD on PSII, we incubated isolated thylakoid membranes separately with both chemicals, applying concentrations that have been earlier used for $^1O_2$ measurements [31,32]. Both compounds rapidly inactivated oxygen evolution and after 5-min incubation in the dark, oxygen evolving activity had decreased by one third in both 10 mM TEMP and 100 mM TEMPD (Fig. 2A). Gradual loss of oxygen evolution occurred during further incubation, and 100 mM TEMPD caused faster loss of PSII activity than 10 mM TEMP (Fig. 2A). Loss of oxygen evolution was accompanied by somewhat slower decrease in F_V/F_M (Fig. 2B).

To understand how TEMP and TEMPD inhibit PSII, we measured the decay of Chl *a* fluorescence yield after a single turnover flash to probe electron transfer from the Q_A electron acceptor of PSII to the secondary quinone Q_B. Incubation of thylakoids with either of the two compounds caused decrease in the rate of the decay of the fluorescence yield (Fig. 3A and B). Both TEMP and TEMPD exerted their effect on Q_A–Q_B electron transfer immediately, as fluorescence curves measured after 10 s of addition of the compounds were virtually identical with curves measured after 30 min of incubation (Fig. 3A and B).

The decay of fluorescence yield was analyzed using a model in which PSII occurred in five states according to the state and functionality of the Q_B site. The model showed a reasonable fit to experimental data (Fig. S1), and the analysis revealed that both TEMP and TEMPD caused a dramatic increase in the proportion of inactive PSII centers from 5% to 19–23% in TEMP and to 27% in TEMPD (Table 1). Both compounds also caused decrease in the number of PSII centers in which the Q_B site is occupied by an oxidized quinone. TEMPD also lowered the rate constant of electron transfer from Q_A^- to Q_B and caused increase in the relative proportion of PSII centers originally in Q_B^- state (Table 1). The larger proportion of PSII centers with Q_B^- was confirmed by adding DCMU to dark adapted thylakoids. This test indicated that the rapid phase of DCMU-induced increase in

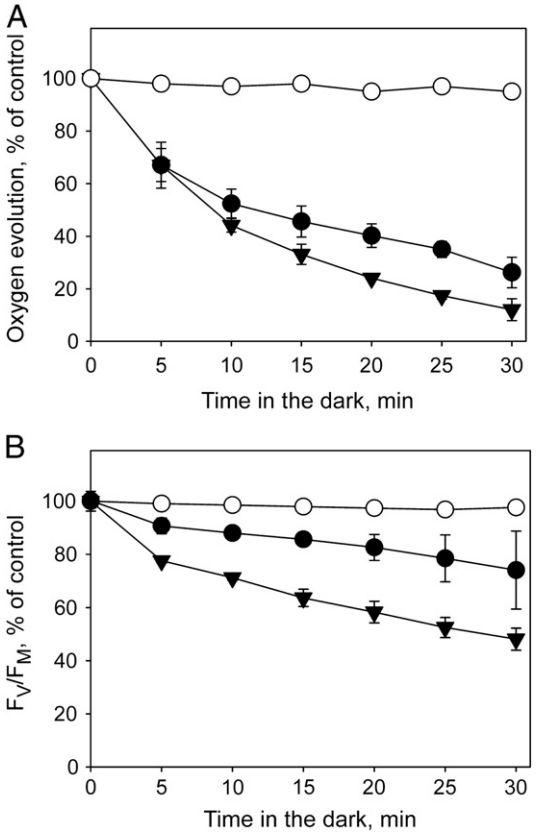

Fig. 2. Loss of oxygen evolution (A) and decrease in F_V/F_M (B) during incubation of thylakoid membranes in the presence of 10 mM TEMP (squares) and 100 mM TEMPD (triangles). Open symbols are measurements from untreated thylakoids. Each data point represents an average of three independent incubations and the error bars show SD. Oxygen evolution was measured using DCBQ as electron acceptor and F_V/F_M was measured with a PAM-101 fluorometer. In control thylakoids, the oxygen evolution rate was 297 ± 29 μmol O_2 (mg Chl)$^{-1}$ h^{-1} and F_V/F_M was 0.73 ± 0.01.

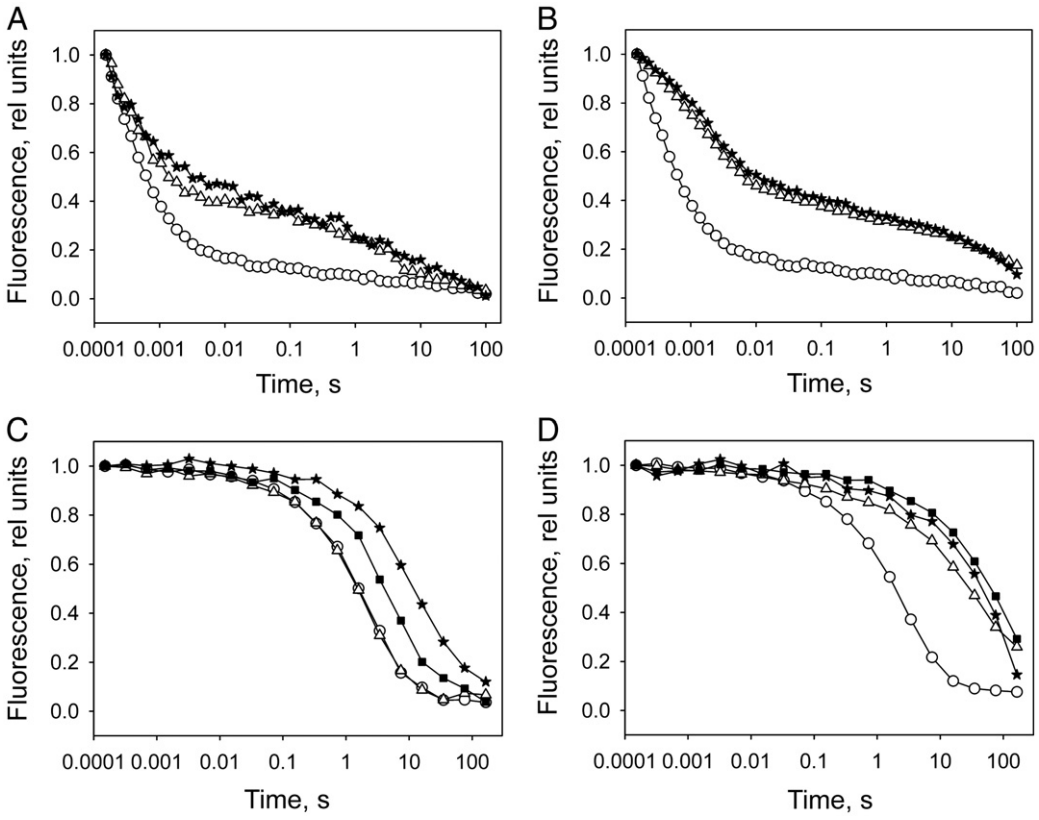

Fig. 3. Effects of 10 mM TEMP (A, C) and 100 mM TEMPD (B, D) on the decay of Chl *a* fluorescence yield after a single turnover flash measured in the absence (A, B) and presence (C, D) of 10 μM DCMU. Thylakoid membranes (20 μg Chl ml^{-1}) were dark adapted for 3 min, a control measurement was done (open circles), and TEMP or TEMPD, as indicated, was added in the dark. The first measurement was initiated 10 s after the addition (open triangles); then thylakoids were incubated in the cuvette of the fluorometer in darkness, except for the measuring flashes and one single turnover flash per measurement, and further measurements were done after 15 min (solid squares) and 30 min incubation (stars). The 15-min curves were omitted from A and B for clarity. All curves have been normalized to make variable fluorescence equal 1.0.

F_0 fluorescence was slightly higher in the presence of 100 mM TEMPD than in control thylakoids (Fig. S2). Three to 4% of variable fluorescence yield was not resolved with the 160 s long measurement. At least in the control thylakoids, this ultra slow fluorescence decay component likely reflects the equilibrium constant of the reaction $Q_A^-Q_B \leftrightarrow Q_AQ_B^-$ [39], as the initial concentration of Q_B^- was near zero (Table 1).

Charge recombination reactions between the quinone electron acceptors Q_A and Q_B and the S_2 state of the oxygen evolving complex are thought to be a source of triplet Chl that causes production of $^1O_2$ in PSII [15,17]. To probe the reaction $S_2Q_A^- \rightarrow S_1Q_A$, we measured the decay of fluorescence yield in the presence of DCMU that blocks electron transfer from Q_A to Q_B. These measurements showed a decrease in the rate of the decay of fluorescence yield (Fig. 3C and D). The effect of TEMP advanced during 30-min incubation whereas TEMPD exerted its effect immediately. The fluorescence data were analyzed according to the three-reaction, two-PSII-population model of Rappaport et al. [35,36] but applying the Eyring theory of reaction rates instead of the Arrhenius equation. The model fitted the experimental data fairly well (Fig. S2), and the analysis showed that both TEMP and TEMPD caused an increase in the half time of $S_2Q_A^-$ recombination of the major, slowly recombining PSII population, from 3 s to 9 s in 10 mM TEMP (30 min incubation) and to 90 s in 100 mM TEMPD (15 min incubation) (Table 2). The half-time of $S_2Q_A^-$ recombination increased also in the minor, rapidly recombining PSII population (Table 2).

To assign the effects of TEMP and TEMPD to the different pathways of the reaction $S_2Q_A^- \rightarrow S_1Q_A$, we measured TL glow curves from TEMP and TEMPD treated thylakoids. TL measurements in the presence of DCMU showed that TEMP caused a 4 °C shift and TEMPD caused an 11 °C shift of the Q band toward higher temperature, suggesting that both compounds cause an increase in the activation free energy of the charge recombination $S_2Q_A^- \rightarrow S_1Q_A$ (Fig. 4A and B). The shift occurred immediately upon addition of TEMP or TEMPD. The amplitude of the Q

Table 1
Analysis of the decay of Chl *a* fluorescence yield after a single turnover flash in the absence of DCMU. The model used in the analysis consisted of electron transfer reactions for PSII centers with Q_B and those with Q_B^-, a Q_B binding reaction (empty site → site with Q_B) and a release reaction (Q_B^{2-} → empty site). A correction was done for the energetic connectivity of PSII according to Eq. (4). In addition, an inactive, slowly decaying fraction of PSII centers was assumed. A small fraction of fluorescence remained unresolved by the model.

	Q_B, %	Q_B^-, %	Empty Q_B site, %	Q_B^{2-}, %	Inact, %	$t_{1/2}$, Q_B to Q_B^-, μs	$t_{1/2}$, Q_B^- to Q_B^{2-}, ms	$t_{1/2}$, binding of Q_B, ms	$t_{1/2}$, release of Q_B^{2-}, s	$t_{1/2}$, Inact, s	Un-resolved, %
Control	73	7	2	9	5	270	2	7	0.25	12	3
TEMP, 10 s	57	3	7	9	22	290	2	7	0.25	6	3
TEMP, 15 min	49	0	16	9	23	250	2	7	0.35	12	3
TEMP, 30 min	53	0	15	9	19	250	2	5	0.33	13	3
TEMPD, 10 s	25	20	13	11	27	640	2	5	0.23	51	4
TEMPD, 15 min	25	20	13	11	27	640	2	5	0.23	51	4
TEMPD, 30 min	25	20	13	11	27	640	2	5	0.23	51	4

Table 2
Analysis of the decay of Chl *a* fluorescence yield after a single turnover flash in the presence of DCMU. The connectivity parameter was fixed at $J=1$.

	Slow PSII population		Fast PSII population		Stable fluorescence, %
	% of PSII	$t_{1/2}$, s	% of PSII	$t_{1/2}$, s	
Control	67	3.0	29	0.35	4
TEMP, 10 s	69	3.8	29	0.43	2
TEMP, 15 min	67	9.2	29	1.0	4
TEMP, 30 min	64	21	27	2.3	9
TEMPD, 10 s	69	25	25	0.09	6
TEMPD, 15 min	86	90	12	1.4	2
TEMPD, 30 min	86	77	12	1.3	2

band progressively decreased during incubation with TEMP and with TEMPD (Fig. 4A and B).

The TL data were modeled to calculate how the two chemicals affected the three different recombination pathways of the two PSII populations [35,36]. The modeling led to a good fit to the experimental data (Fig. S4). The analysis revealed that the decrease in the amplitude of the Q band during incubation with TEMP or TEMPD was caused by decrease in the number of active PSII centers (Fig. 2), not by a specific decrease in the yield of the excitonic pathway (Table 3). This conclusion is in agreement with the finding that the decay of Chl *a* fluorescence yield after a single turnover flash in the presence of DCMU also slowed down during treatment with TEMP or TEMPD (Fig. 3). The best fit of TL data was obtained by allowing the $\Delta H^{\ddagger}$ values of all three pathways of the major, slowly recombining PSII population to increase during incubation with TEMP or TEMPD, suggesting that both compounds cause an increase in the redox potential of the Q_A/Q_A^- pair, i.e. stabilize the $S_2Q_A^-$ state. Incubation with TEMP had only a minor effect on the activation parameters of the fast PSII population but TEMPD treatment caused a large increase in the $\Delta H^{\ddagger}$ values of $S_2Q_A^-$ recombination reactions of the fast PSII population, too (Table 3). The fits did not suggest changes in $\Delta S^{\ddagger}$ values, and therefore the increase in $\Delta G^{\ddagger}$ was entirely due to increase in $\Delta H^{\ddagger}$. The increase in the rate constant of the recombination reaction (Eq. (2)) of the slow PSII population (Table 3) was smaller than in the fluorescence data (Table 2).

To measure potential effects on the Q_B quinone, we also measured the TL B band that reflects the recombination reaction $S_2Q_B^- \rightarrow S_1Q_B$. TEMPD caused an immediate 10 °C shift of the peak position of the B band to a lower temperature while TEMP caused a smaller, gradual shift of up to 4 °C during the 30-min incubation. Analysis of the B band (Fig. S5) showed that $\Delta G^{\ddagger}$ of $S_2Q_B^-$ recombination decreased by 12 meV during incubation with TEMP and by 27 meV when TEMPD was used (Table 4). Incubation of thylakoids with 10 mM TEMP caused a moderate decrease in the amplitude of the B band, similar to the decrease of the Q band caused by the same compound (Fig. 4C), whereas TEMPD caused a rapid decrease of the B band to one fifth of the control amplitude (Fig. 4D). During further incubation with TEMPD, the B band almost disappeared.

4. Discussion

$^1O_2$ is an often harmful reactive oxygen species [41,42] that can be detected with substances that react specifically with $^1O_2$, producing spectroscopically detectable products [4–9,31,32]; see [42] for review. However, before using $^1O_2$ indicators, it is essential to measure the direct effects of the indicator on the biological activity of the sample. $^1O_2$ sensor compounds must be treated with special care, as artifacts are easy to obtain in $^1O_2$ research. For example, the commercially available compound Singlet Oxygen Sensor Green

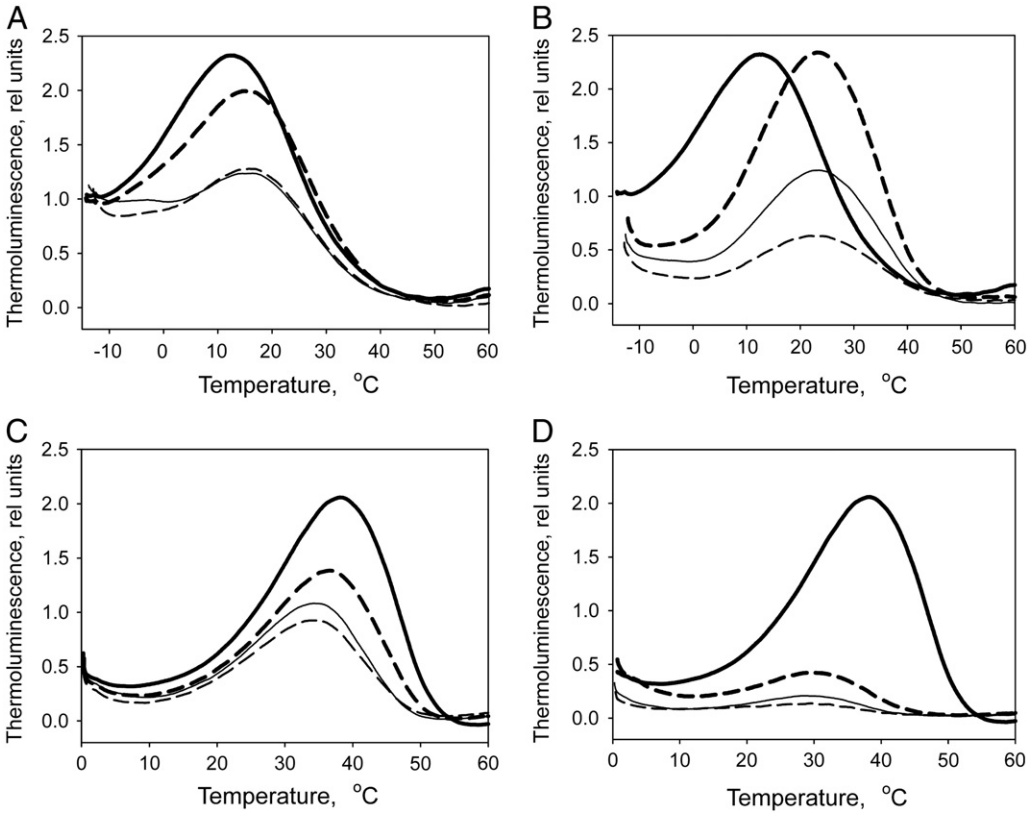

Fig. 4. Effect of 10 mM TEMP (A, C) and 100 mM TEMPD (B, D) on the Q band of TL, measured in the presence of 20 μM DCMU (A, B) and on B band of TL, measured in the absence of DCMU (C, D). Thick solid line, control; thick dashed line, measurement after 10 s of addition of TEMP or TEMPD; thin solid line and thin dashed line, measurement after 15 and 30 min, respectively after addition of TEMP or TEMPD.

Table 3
Analysis of the Q band of TL. The connectivity parameter J had the value 1.0. $\Delta H^{\ddagger}$ (meV) values are common to both PSII populations. 70% of PSII belonged to the slow, characterized by $\Delta S^{\ddagger}_{j} = -0.58$ meV/K, $\Delta S^{\ddagger}_{exc} = -0.79$ meV/K and $\Delta S^{\ddagger}_{d} = -2.1$ meV/K and 30% to the fast PSII population characterized by $\Delta S^{\ddagger}_{j} = -0.4$ meV/K, $\Delta S^{\ddagger}_{exc} = -0.8$ meV/K and $\Delta S^{\ddagger}_{d} = -1.9$ meV/K. $\Delta G^{\ddagger}$ values are calculated at 25 °C. Peak amplitude (Amp.) and the modelled amount of recombining $S_2Q_A^-$ (Act.) are also shown. The half-time ($t_{1/2}$) values are in seconds.

	Peak temp., °C	Amp., % of control	Act.,% of control	$\Delta H^{\ddagger}_{i}$	$\Delta H^{\ddagger}_{exc}$	$\Delta H^{\ddagger}_{d}$	Slow PSII population				Fast PSII population			
							$\Delta G^{\ddagger}_{i}$	$\Delta G^{\ddagger}_{exc}$	$\Delta G^{\ddagger}_{d}$	$t_{1/2}$	$\Delta G^{\ddagger}_{i}$	$\Delta G^{\ddagger}_{exc}$	$\Delta G^{\ddagger}_{d}$	$t_{1/2}$
Control	12.4	100	100	638	666	198	809	899	818	3.5	756	902	759	0.40
TEMP, 10 s[a]	15.0	86	49	642	662	204	813	895	824	4.2	760	898	765	0.49
TEMP, 15 min	16.0	53	42	642	670	204	813	903	824	4.2	760	906	765	0.49
TEMP, 30 min	16.0	55	43	642	670	204	813	903	824	4.2	760	906	765	0.49
TEMPD, 10 s[a]	23.1	100	95	652	701	224	823	934	844	7.2	770	937	785	0.40
TEMPD, 15 min	23.1	54	50	652	701	224	823	934	844	7.2	770	937	785	0.83
TEMPD, 30 min	23.1	27	25	652	701	224	823	934	844	7.2	770	937	785	0.83

[a] Approximately 1 min was required to cool the sample from room temperature to −15 °C.

(Invitrogen, Inc., Carlsbad, CA, USA) shows a strong fluorescence signal if illuminated with wavelengths below 650 nm in the absence of $^1O_2$ sensitizers (Fig. S6). Furthermore, although this compound functions well when methylene blue is used as a sensitizer, the small signal obtained with thylakoids is not sensitive to use of deuterium oxide, anaerobicity or azide (Fig. S7).

We studied the effects of two $^1O_2$ sensor substances, TEMP and TEMPD. Both produce an N-oxyl derivative in reaction with $^1O_2$, and the derivative can be quantified with magnetic resonance spectroscopy. TEMP and TEMPD were found to have two types of effects on PSII. Firstly, TEMP and TEMPD caused a rapid major change in the properties of the acceptor side of PSII, characterized by stabilization of Q_A^- (Fig. 3A and B; Tables 2 and 3), destabilization of Q_B^- (Fig. 3C and D; Table 4) and slowing down of electron transfer from Q_A to Q_B (Table 1). Secondly, loss of the number of active PSII units advanced during 30 min incubation of thylakoids with TEMP and with TEMPD. This secondary effect is evidenced by decrease in the oxygen evolution activity and F_V/F_M (Fig. 2) and in the amplitudes of both TL bands (Fig. 4). Loss of oxygen evolution capacity and decrease in TL amplitudes show correlation with each other (Fig. S8). The effects on the redox potentials partially explain the decrease in oxygen evolution, as the difference in redox midpoint potential between the Q_A/Q_A^- and Q_B/Q_B^- redox couples is the driving force of electron transfer from Q_A to the plastoquinone pool. Due to opposite changes in $\Delta G^{\ddagger}$ values (increase of $\Delta G^{\ddagger}$ of all three routes of $S_2Q_A^- \rightarrow S_1Q_A$ recombination in both PSII populations and decrease of $\Delta G^{\ddagger}$ of $S_2Q_B^- \rightarrow S_1Q_B$), the redox potential difference decreased radically. If the redox potential difference between Q_A/Q_A^- and Q_B/Q_B^- is calculated using the $\Delta G^{\ddagger}$ of the main (indirect) pathway of the main (slow) PSII population, then the redox potential difference decreases from the control value of 42 mV to 26 mV during incubation with TEMP and to 2 mV in thylakoids incubated with TEMPD (Tables 3 and 4). Accordingly, TEMPD inhibited oxygen evolution more severely than TEMP (Fig. 2).

Compounds modifying the environment of the quinones have earlier shown to affect the redox potentials. Ureas like DCMU, certain phenolic compounds like phenmedipham, bromoxynil and dinoseb, and triazines like atrazine bind to the Q_B site and simultaneously change the redox potential of the Q_A/Q_A^- couple [43,44]. For example, the binding of bromoxynil and dinoseb destabilizes the $S_2Q_A^-$ state by a factor of 10, compared to the stability of this state in the presence of DCMU [44]. Furthermore, D1 protein mutants have revealed that the redox potentials of the quinone electron acceptors are sensitive to changes in the protein environment [45–47]. These data suggest that TEMP and TEMPD may act by interacting with the reaction centre proteins of PSII.

The finding that both TEMP and TEMPD modify the activation parameters of the $S_2Q_A^-$ and $S_2Q_B^-$ charge recombination reactions may suggest that these compounds are not suitable for $^1O_2$ determination in photosynthetic systems. The observed effects on PSII charge recombination reactions most probably affect the probability of $^1O_2$ production by PSII, as charge recombination is an important route of triplet Chl formation [10,15,48,49]. Results obtained by using TEMP and TEMPD must be interpreted with care, taking into account the side effects.

The present results may have importance with regard to photoinhibition of PSII. Some of the key studies that showed the importance of $^1O_2$ in photoinhibition have been conducted using TEMP [4,5,31], and more recently also TEMPD has been used [32]. The validity of the conclusions of these studies, especially regarding the role of the PSII charge recombination reactions in $^1O_2$ production, can be questioned, as both indicator chemicals have strong effects on the recombination reactions. Thus, the question of the role of $^1O_2$ in photoinhibition may require reconsideration. It should be noted, however, that TEMP or TEMPD have not been used in all experiments probing the importance of $^1O_2$ in photoinhibition. The criticism presented here may not apply to other $^1O_2$ indicator chemicals like dansyl-2,2,5,5-tetramethyl-2,5-dihydro-1*H*-pyrrole (DanePy) [6]. DanePy detects $^1O_2$ via a similar nitroxide formation reaction as TEMP [6], but the $^1O_2$-reactive moiety of DanePy is a tetramethylpyrrole rather than a tetramethylpiperidine.

Apart from its suggested role in the reaction mechanism of photoinhibition, $^1O_2$ inhibits translation elongation in cyanobacteria [50], thus interfering with the repair of photoinhibited PSII. There is evidence suggesting that inhibition of the repair is the only significant contribution of $^1O_2$ in photoinhibition [11,50,51] but conflicting

Table 4
Analysis of the B band of TL. $\Delta H^{\ddagger}$ and $\Delta S^{\ddagger}$ are the activation enthalpy and activation entropy of the recombination reaction, respectively. $\Delta G^{\ddagger}$ and the half-time ($t_{1/2}$) are calculated at 25 °C.

Treatment	Peak temperature, °C	Amplitude, % of control	$\Delta H^{\ddagger}$, meV	$\Delta S^{\ddagger}$, meV K^{-1}	$\Delta G^{\ddagger}$, meV	$t_{1/2}$, s
Control	38.0	100	908	0.19	851	28
TEMP, 10 s[a]	36.4	67	903	0.19	846	23
TEMP, 15 min	34.3	52	897	0.19	840	18
TEMP, 30 min	34.1	45	896	0.19	839	18
TEMPD, 10 s[a]	28.1	22	786	−0.13	825	9.9
TEMPD, 15 min	28.5	11	786	−0.13	825	9.9
TEMPD, 30 min	27.1	7	786	−0.13	825	9.9

[a] Approximately 40 s was required to cool the sample from room temperature to 0 °C.

results have been obtained about direct inhibition of PSII by $^1O_2$ produced by sensitizer chemicals [50,52]. Thus, more research is needed to elucidate the role of $^1O_2$ in photoinhibition. It should also be noted that contribution of reactive oxygen species in the mechanism by which light absorption by manganese ions causes the loss of oxygen-evolution activity [13,22,23] cannot be ruled out.

The present data do not resolve the mechanism of the decrease in PSII oxygen evolution activity, variable fluorescence and thermoluminescence amplitude occurring during incubation of TEMP or TEMPD with a time constant of 5–15 min (Figs. 2 and 4). We consider it possible that the nitrogen of the piperidine ring may react with a component of the PSII electron transfer chain but the reaction is slow because the component is protected by the protein matrix.

In conclusion, our experiments reveal unexpected, severe effects on PSII electron transfer reactions by two $^1O_2$ sensor compounds. Further research is needed to find out whether the effects are due to the reactivity of the nitrogen that also reacts with oxygen, or whether PSII is inhibited due to some other common property of TEMP and TEMPD. Anyway, the results indicate that thorough tests for side effects of sensor chemicals are of great importance before they are used for detection of $^1O_2$.

Acknowledgments

Heta Mattila is thanked for help with the experiments. Academy of Finland and Finnish Cultural Foundation are acknowledged for funding of this study.

Appendix A. Supplementary data

Supplementary data to this article can be found online at doi:10.1016/j.bbabio.2010.11.014.

References

[1] L.-Y. Zang, F.J.G.M. van Kuijk, B.R. Misra, H.P. Misra, The specificity and product of quenching singlet oxygen by 2, 2, 6, 6-tetramethylpiperidine, Biochem. Mol. Biol. Int. 37 (1995) 283–293.
[2] T. Vogler, A. Studer, Applications of TEMPO in synthesis, Synthesis 13 (2008) 1979–1993.
[3] C.S. Wilcox, Effects of Tempol and redox-cycling nitroxides in models of oxidative stress, Pharmacol. Ther. 126 (2010) 119–145.
[4] É. Hideg, I. Spetea, Vass, Singlet oxygen production in thylakoid membranes during photoinhibition as detected by EPR spectroscopy, Photosynth. Res. 39 (1994) 191–199.
[5] É. Hideg, C. Spetea, I. Vass, Singlet oxygen and free-radical production during acceptor- and donor-side-induced photoinhibition. Studies with spin trapping EPR spectroscopy, Biochim. Biophys. Acta 1186 (1994) 143–152.
[6] É. Hideg, T. Kálai, K. Hideg, I. Vass, Photoinhibition of photosynthesis in vivo results in singlet oxygen production detection via nitroxide-induced fluorescence in broad bean leaves, Biochemistry 37 (1998) 11405–11411.
[7] É. Hideg, K. Ogawa, T. Kálai, K. Hideg, Singlet oxygen imaging in *Arabidopsis thaliana* leaves under photoinhibition by excess photosynthetically active radiation, Physiol. Plant. 112 (2001) 10–14.
[8] É. Hideg, C. Barta, T. Kálai, I. Vass, K. Hideg, K. Asada, Detection of singlet oxygen and superoxide with fluorescent sensors in leaves under stress by photoinhibition or UV radiation, Plant Cell Physiol. 43 (2002) 1154–1164.
[9] C. Barta, T. Kalai, K. Hideg, I. Vass, É. Hideg, Differences in the ROS-generating efficacy of various ultraviolet wavelengths in detached spinach leaves, Func. Plant Biol. 31 (2004) 23–28.
[10] A. Krieger-Liszkay, C. Fufezan, A. Trebst, Singlet oxygen production in photosystem II and related protection mechanism, Photosynth. Res. 98 (2008) 551–564.
[11] Y. Nishiyama, S.I. Allakhverdiev, N. Murata, A new paradigm for the action of reactive oxygen species in the photoinhibition of photosystem II, Biochim. Biophys. Acta 1757 (2006) 742–749.
[12] N. Murata, S. Takahashi, Y. Nishiyama, S.I. Allakhverdiev, Photoinhibition of photosystem II under environmental stress, Biochim. Biophys. Acta 1767 (2007) 414–421.
[13] E. Tyystjärvi, Photoinhibition and photodamage of the oxygen evolving manganese cluster, Coord. Chem. Rev. 252 (2008) 361–376.
[14] I. Vass, E.-M. Aro, Photoinhibition of Photosystem II electron transport, in: G. Renger (Ed.), Primary Processes of Photosynthesis: Basic Principles and Apparatus. Comprehensive Series in Photochemical and Photobiological Sciences, Vol. 8, Publications of the Royal Society of Chemistry, Cambridge, 2008, pp. 393–411.
[15] I. Vass, S. Styring, T. Hundal, A. Koivuniemi, E.-M. Aro, B. Andersson, Reversible and irreversible intermediates during photoinhibition of photosystem II. Stable reduced QA species promote chlorophyll triplet formation, Proc. Nat. Acad. Sci. U.S.A. 89 (1992) 1408–1412.
[16] L. Nedbal, G. Samson, J. Whitmarsh, Redox state of a one-electron component controls the rate of photoinhibition of photosystem II, Proc. Natl Acad. Sci. USA 89 (1992) 7929–7933.
[17] N. Keren, A. Berg, P.J.M. van Kan, H. Levanon, I. Ohad, Mechanism of photosystem II photoinactivation and DI protein degradation at low light: the role of back electron flow, Proc. Nat. Acad. Sci. U. S. A. 94 (1997) 1579–1584.
[18] S. Santabarbara, I. Cazzalini, A. Rivadossi, F.M. Garlaschi, G. Zucchelli, R.C. Jennings, Photoinhibition *in vivo* and *in vitro* involves weakly coupled chlorophyll-protein complexes, Photochem. Photobiol. 75 (2002) 613–618.
[19] J. Jung, H.S. Kim, The chromatophores as endogenous sensitizers involved in the photogeneration of singlet oxygen in spinach thylakoids, Photochem. Photobiol. 52 (1990) 1003–1009.
[20] G.-X. Chen, J. Kazimir, G.M. Cheniae, Photoinhibition of hydroxylamine-extracted photosystem II membranes: studies of the mechanism, Biochemistry 31 (1992) 11072–11083.
[21] J.M. Anderson, Y.-I. Park, W.S. Chow, Unifying model for the photoinactivation of photosystem II in vivo: a hypothesis, Photosynth. Res. 56 (1998) 1–13.
[22] M. Hakala, I. Tuominen, M. Keränen, T. Tyystjärvi, E. Tyystjärvi, Evidence for the role of the oxygen-evolving manganese complex in photoinhibition of Photosystem II, Biochim. Biophys. Acta 1706 (2005) 68–80.
[23] N. Ohnishi, S.I. Allakhverdiev, S. Takahashi, S. Higashi, M. Watanabe, Y. Nishiyama, N. Murata, Two-step mechanism of photodamage to Photosystem II: Step 1 occurs at the oxygen-evolving complex and step 2 occurs at the photochemical reaction center, Biochemistry 44 (2005) 8494–8499.
[24] E. Tyystjärvi, N. King, M. Hakala, E.-M. Aro, Artificial quenchers of chlorophyll fluorescence do not protect against photoinhibition, J Photochem. Photobiol. B Biol. 48 (1999) 142–147.
[25] P. Sarvikas, M. Hakala, E. Pätsikkä, T. Tyystjärvi, E. Tyystjärvi, Action spectrum of photoinhibition in leaves of wild type and *npq1-2* and *npq4-1* mutants of *Arabidopsis thaliana*, Plant Cell Physiol. 47 (2006) 391–400.
[26] O. Zsiros, S.I. Allakhverdiev, S. Higashi, M. Watanabe, Y. Nishiyama, N. Murata, Very strong UV-A light temporally separates the photoinhibition of photosystem II into light-induced inactivation and repair, Biochim. Biophys. Acta 1757 (2006) 123–129.
[27] M. Hakala-Yatkin, M. Mäntysaari, H. Mattila, E. Tyystjärvi, Contributions of visible and ultraviolet parts of sunlight to photoinhibition, Plant Cell Physiol. 51 (2010) 1745–1753.
[28] P. Sarvikas, M. Hakala-Yatkin, S. Dönmez, E. Tyystjärvi, Short flashes and continuous light have similar photoinhibitory efficiency in intact leaves, J. Exp. Bot. 61 (2010) 4239–4247.
[29] M. Hakala, S. Rantamäki, E.-M. Puputti, T. Tyystjärvi, E. Tyystjärvi, Photoinhibition of manganese enzymes – insights into the mechanism of Photosystem II photoinhibition, J. Exp. Bot. 57 (2006) 1809–1816.
[30] T.K. Antal, W. Lo, W.H. Armstrong, E. Tyystjärvi, Illumination with ultraviolet or visible light induces chemical changes in the water-soluble manganese complex, $[Mn_4O_6(bpea)_4]Br_4$, Photochem. Photobiol. 85 (2009) 663–668.
[31] C. Fufezan, A.W. Rutherford, A. Krieger-Liszkay, Singlet oxygen production in herbicide-treated photosystem II, FEBS Lett. 532 (2002) 407–410.
[32] B.B. Fischer, A. Krieger-Liszkay, É. Hideg, I. Snyrychova, M. Wiesendanger, R.I.L. Eggen, Role of singlet oxygen in chloroplast to nucleus retrograde signaling in *Chlamydomonas reinhardtii*, FEBS Lett. 581 (2007) 5555–5560.
[33] E. Tyystjärvi, S. Rantamäki, J. Tyystjärvi, Connectivity of Photosystem II is the physical basis of retrapping in photosynthetic thermoluminescence, Biophys. J. 96 (2009) 3735–3743.
[34] J.-M. Ducruet, I. Vass, Thermoluminescence: experimental, Photosynth. Res. 101 (2009) 195–204.
[35] F. Rappaport, J. Lavergne, Thermoluminescence: theory, Photosynth. Res. 101 (2009) 205–216.
[36] F. Rappaport, A. Cuni, L. Xiong, R. Sayre, J. Lavergne, Charge recombination and thermoluminescence in photosystem II, Biophys. J. 88 (2005) 1948–1958.
[37] S. Glasstone, K.J. Laidler, H. Eyring, The Theory of Rate Processes, McGraw-Hill Company, New York, 1941.
[38] J. Lavergne, H.W. Trissl, Theory of fluorescence induction in photosystem II: derivation of analytical expressions in a model including exciton-radical pair equilibrium and restricted energy transfer between photosynthetic units, Biophys. J. 68 (1995) 2474–2492.
[39] G. Renger, H.-J. Eckert, A. Bergmann, J. Bernarding, B. Liu, A. Napiwotzki, F. Reifarth, H.J. Eichler, Fluorescence and spectroscopic studies of exciton trapping and electron transfer in Photosystem II of higher plants, Aust. J. Plant Physiol. 22 (1995) 167–181.
[40] E. Tyystjärvi, I. Vass, Light Emission as a Probe of Charge Separation and Recombination in the Photosynthetic Apparatus: Relation of Prompt Fluorescence to Delayed Light Emission and Thermoluminescence, in: G.C. Papageorgiou, Govindjee (Eds.), Chlorophyll *a* Fluorescence: A Signature of Photosynthesis. Series: Advances in Photosynthesis and Respiration, Vol. 19, Kluwer Academic Publishers, Dordrecht, 2004, pp. 363–388.
[41] B. Halliwell, J.M.C. Gutteridge, Free Radicals in Biology and Medicine, Oxford University Press, Oxford, 1999.
[42] G. Schweitzer, R. Schmidt, Physical mechanisms of generation and deactivation of singlet oxygen, Chem. Rev. 103 (2003) 1685–1757.
[43] S. Demeter, M. Droppa, I. Vass, G. Horvath, The thermo-luminescence of chloroplasts in the presence of Photosystem-II herbicides, Photobiochem. Photobiophys. 4 (1982) 163–168.

[44] A.G. Roberts, W. Gregor, R.D. Britt, D.M. Kramer, Acceptor and donor-side interactions of phenolic inhibitors in Photosystem II, Biochim. Biophys. Acta 1604 (2003) 23–32.
[45] H.M. Gleiter, N. Ohad, H. Koike, J. Hirschberg, G. Renger, Y. Inoue, Thermoluminescence and flash-induced oxygen yield in herbicide resistant mutants of the D1 protein in *Synechococcus* PCC7942, Biochim. Biophys. Acta 1140 (1992) 135–143.
[46] P. Mäenpää, T. Miranda, E. Tyystjärvi, T. Tyystjärvi, Govindjee, J.-M. Ducruet, A.-L. Etienne, D. Kirilovsky, A mutation in the D-*de* loop of D_1 modifies the stability of the $S_2Q_{\overline{A}}$ and $S_2Q_{\overline{B}}$ states in Photosystem II, Plant Physiol. 107 (1995) 187–197.
[47] M. Keränen, P. Mulo, E.-M. Aro, Govindjee, E. Tyystjärvi, Thermoluminescence B and Q bands are at the same temperature in an autotrophic and a heterotrophic D1 protein mutant of *Synechocystis* sp. PCC 6803, in: G. Garab (Ed.), Photosynthesis: Mechanisms and Effects, Vol II, Kluwer Academic Publishers, Dordrecht, 1998, pp. 1145–1148.
[48] N. Keren, I. Ohad, A.W. Rutherford, F. Drepper, A. Krieger-Liszkay, Inhibition of photosystem II activity by saturating single turnover flashes in calcium-depleted and active photosystem II, Photosynth. Res. 63 (2000) 209–216.
[49] I. Vass, K. Cser, Janus-faced charge recombinations in photosystem II photoinhibition, Trends Plant Sci. 14 (2009) 200–205.
[50] Y. Nishiyama, S.I. Allakhverdiev, H. Yamamoto, H. Hayashi, N. Murata, Singlet oxygen inhibits the repair of Photosystem II by suppressing the translation elongation of the D1 protein in *Synechocystis* sp. PCC 6803, Biochemistry 43 (2004) 11321–11330.
[51] S. Inoue, K. Ejima, E. Iwai, H. Hayashi, J. Appel, E. Tyystjärvi, N. Murata, Y. Nishiyama, Protection by α-tocopherol of the repair of photosystem II during photoinhibition in *Synechocystis* sp. PCC 6803, Biochim. Biophys. Acta 1807 (2011) 236–241.
[52] É. Hideg, P. Kós, I. Vass, Photosystem II damage induced by chemically generated singlet oxygen in tobacco leaves, Physiol. Plant. 131 (2007) 33–40.